

# STRESS DIAGNOSIS METHOD BASED ON THE SECTION FLATNESS OF A BENT PIPE

S. Imura

Tokyo Gas Co., LTD., Tokyo, Japan

**Abstract:** If ground subsidence or seismic load acts on piping that includes bent pipes, the highest stress often occurs not in a straight section but in a bent section. The author has therefore developed a method of estimating the stress generated by a change in diameter by adding an equation for the diameter change and bending moment to the bent pipe stress calculation equations proposed by Rodabaugh and George. To investigate the validity of this method, two kinds of bent pipe made using typical bent pipe manufacturing methods and having representative section wall thickness distributions were tested to determine the relationship between the diameter change and the stress generated when in-plane bending moment is applied. As a result, it was confirmed that the stress estimated from the diameter change closely agrees with the measured value.

**Introduction:** It is essential to determine the stress generated in pipelines in order to maintain their safety against external forces, and to do so by non-destructive diagnosis for pipelines that are in service. However, the method involves measuring deformation after installing strain gauges, so it is impossible to diagnose stress over time unless strain gauges are installed when the pipelines are laid. One common method is to use pipe deflection indicators[1] to measure pipeline deformation and to enter deformation readings into an FEM program to calculate the stress, but this is not a very precise method.

Bent pipes are generally used in pipelines extending across rivers and at the entrances to multi-purpose utility tunnels, and the highest stresses often occur not in straight sections but in bent sections. Imura and Sakai have developed a method of non-destructively measuring stresses occurring in bent pipes using the principle of magnetostriction[2]. The values measured by the magnetic method were regressed to Von Karman's theoretical stress calculation equation [3] for a bent pipe. From the regression curve obtained, it was possible to obtain only the external force moment that purely applies bending to the pipe. But it has been revealed that if the methods of manufacturing the bent pipes differ, the range where stress can be diagnosed is narrower than that of a straight pipe of the same grade. This means that when the non-destructive diagnosis method developed for welding elbows and for induction pipe bends is applied, the upper limit for application of the former is about 50% of the yield stress. Therefore, a non-destructive stress diagnosis method with a wider range of measurable stress was necessary.

If ground subsidence or seismic load acts on piping that includes bent sections, bending moment acts on the bent sections in almost every case, causing section flatness on the bent pipe. Various formulae have been proposed for calculating the stress distribution when bending moment due to an external force acts on a bent pipe, the best known of which is that proposed by Von Karman[3]. However, in this study, the practicality of estimating stress generated based on the section flatness by extending the method proposed by Rodabaugh & George[4] is investigated.

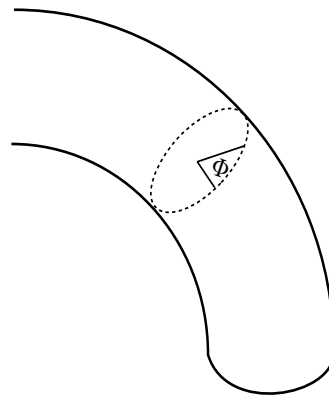


Figure 1: Definition of the angle of a bent pipe.

**Calculating the stress distribution from section flatness:** According to Rodabaugh & George, the longitudinal and circumferential stresses  $\sigma_{iL}$ ,  $\sigma_{iC}$ ,  $\sigma_{oL}$ ,  $\sigma_{oC}$  when in-plane bending moment  $M_i$  and out-of-plane bending moment  $M_o$  act on a bent pipe are represented by the following equations.

$$\begin{aligned}\sigma_{iL} &= \frac{k_p M_i r}{I(1-\nu^2)} f_1(\phi) , & \sigma_{iC} &= \frac{k_p M_i r}{I(1-\nu^2)} f_2(\phi) \\ \sigma_{oL} &= \frac{k_p M_o r}{I(1-\nu^2)} f_3(\phi) , & \sigma_{oC} &= \frac{k_p M_o r}{I(1-\nu^2)} f_4(\phi)\end{aligned}\quad (1)$$

where,  $\phi$  is the circumferential angle of the pipe (see Figure 1),  $\nu$  is Poisson's ratio,  $R$  is the radius of curvature of the bent pipe,  $r$  is the pipe radius,  $t$  is the pipe wall thickness,  $I$  is the geometrical moment of inertia, and  $M$  is the moment acting on the bend.  $k_p$  is called the flexibility factor and substituting it yields a function of  $\lambda$  ( $= tR / r^2 \sqrt{1-\nu^2}$ ) and internal pressure  $P$ . By specifying the stress during the action of in-plane bending moment, the following equations are obtained:

$$\begin{aligned}f_1(\phi) &= (1 + \frac{3d_1}{2}) \sin \phi + \frac{1}{2} \sum_{n=1}^{\infty} \{d_n(1-2n) + d_{n+1}(2n+3)\} \sin(2n+1)\phi \\ &\quad \pm \frac{\nu\lambda}{2} \sum_{n=1}^{\infty} d_n(2n-8n^3) \cos 2n\phi\end{aligned}\quad (2)$$

$$\begin{aligned}f_2(\phi) &= \nu(1 + \frac{3d_1}{2}) \sin \phi + \frac{\nu}{2} \sum_{n=1}^{\infty} \{d_n(1-2n) + d_{n+1}(2n+3)\} \sin(2n+1)\phi \\ &\quad \pm \frac{\lambda}{2} \sum_{n=1}^{\infty} d_n(2n-8n^3) \cos 2n\phi\end{aligned}\quad (3)$$

where  $d_n$  is, like  $k_p$ , a function of  $\lambda$  and internal pressure  $P$ . Regarding which order of term  $n$  should be taken, unlike a case based on the value of  $\lambda$ , the smaller the value of  $\lambda$ , the higher the order of term that is necessary, but if  $\lambda$  is greater than 0.1, up to the third order is appropriate. Therefore,  $d_n$  is represented:

$$\begin{aligned}d_1 &= \frac{3(C_2 C_3 - 110.25)}{6.25C_3 - C_1(C_2 C_3 - 110.25)} \\ d_2 &= \frac{7.5C_3}{6.25C_3 - C_1(C_2 C_3 - 110.25)} \\ d_3 &= \frac{78.75}{6.25C_3 - C_1(C_2 C_3 - 110.25)}\end{aligned}$$

By substituting

$$\begin{aligned}\psi &= PR^2 / Ert \\ C_1 &= 5 + 6\lambda^2 + 24\psi \\ C_2 &= 17 + 600\lambda^2 + 480\psi \\ C_3 &= 37 + 7350\lambda^2 + 2520\psi\end{aligned}$$

Assuming that the maximum section deformation in the radial direction during the action of in-plane bending and out-of-plane bending moment are represented by  $e_i$  and  $e_o$  respectively and expanding the equation for the radial displacement to derive the relationship with the moment  $M$ , we obtain:

$$M_i = \frac{E I e_i}{k_p r R (2d_1 + 4d_2 + 6d_3)} \quad (4)$$

$$M_o = \frac{E I e_o}{k_p r R (2d_1 - 6d_3)} \quad (5)$$

Figure 2 shows the radial displacement distribution during in-plane or out-of-plane bending. The radial displacement of the section during in-plane bending is greatest in the direction where  $0^\circ$  and  $180^\circ$  are linked in Figure 1, the symbols are opposed in the  $90^\circ$  to  $-90^\circ$  directions, and it is smaller than the former. The radial displacement in the section during out-of-plane bending is 0 in the  $0^\circ$ ,  $90^\circ$ ,  $180^\circ$ , and  $-90^\circ$  cases, and maximum at the location where it deviates from this by  $45^\circ$ . Therefore, even during bending in both the in-plane and out-of-plane directions, if flatness  $2e_i$  is measured in the  $0^\circ$  and  $180^\circ$  directions and if flatness  $2e_o$  is measured in the  $45^\circ$  and  $-135^\circ$  directions, then external forces  $M_i$  and  $M_o$  can be calculated from equations (4) and (5), and hence the stress at any location in the section can be calculated from equations (1), (2) and (3).

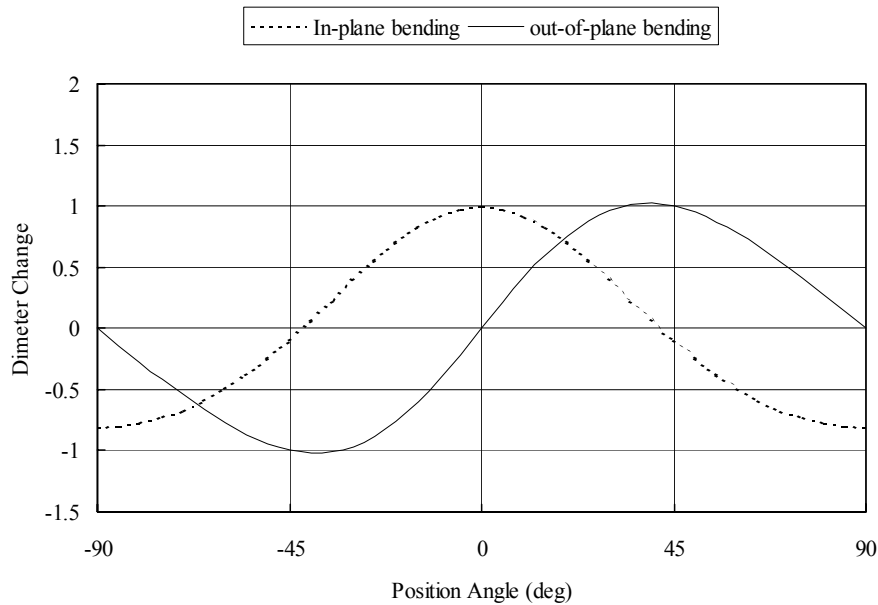


Figure 2: Radial displacement on the center section of a bent pipe during in-pane or out-of-plane bending.

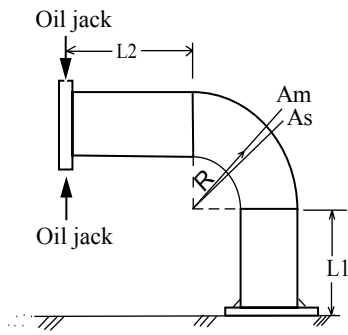


Figure 3: Illustration of experiment.

**Experimental procedure:** Tangent pipes were welded to both sides of the bent pipe, one was attached to the base by a flange, then load was placed on the other flange in the inner bend and the outer bend directions with an oil jack.

The change in the external diameter at the central section of the elbow was measured in two directions with slide calipers. Near the center section, 2-axis strain gauges were installed on the half section at intervals of  $15^\circ$  to verify the results. Figure 3 is a schematic diagram of the test apparatus. The test was performed using the two types of bent pipe shown in Table 1. Figure 4 shows the distribution of bent pipe wall thickness at the centre section.

Table 1. Specimen specifications.

Type	Welded elbow	Induction pipe bend
Material	API-X60	API-X65
External diameter (mm)	610	610
Radius of curvature (mm)	900	1800
Average wall thickness (mm)	17.6	19.1
L1 (mm)	1590	2090
L2 (mm)	1810	2070
$\lambda$	0.189	0.414
Yield stress (MPa)	410	450

A welded elbow is made by pressing two plates then welding them together as shown in Figure 5. In Figure 4, the wall is thick at  $90^\circ$  and at  $-90^\circ$ . This location indicates the weld seam in the longitudinal direction of the pipe.

An induction pipe bend is made by performing high-frequency induction heating of a straight pipe as shown in Figure 6 while bending it to the target aperture angle at the stipulated radius of curvature. Therefore, its wall is inevitably thin on the back side and thick on the front side. The wall is thick at  $-23^\circ$ , but this is also the welding seam in the longitudinal direction.

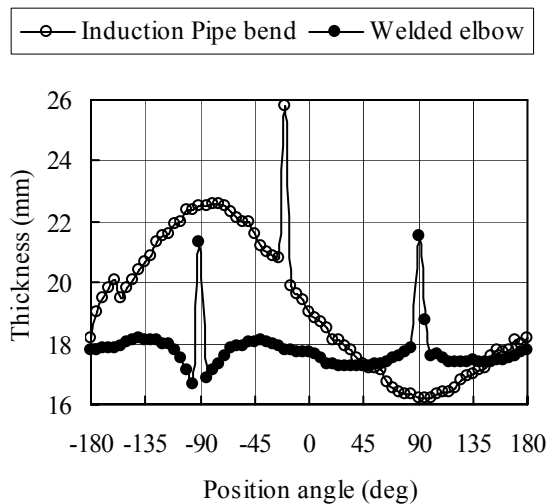


Figure 4: Distribution of pipe wall thickness.

## Results and discussion:

**(a) Welded elbow.** Figure 7 shows the relationship of the magnitude of change of the external diameter of the welded elbow measured with the slide calipers and the maximum stress (circumferential) obtained by the strain gauges. As a welded elbow is made by welding two divided parts in the longitudinal direction (axis of the pipe), it is deformed more easily from  $0^\circ$  to  $180^\circ$  than in the  $90^\circ$  to  $-90^\circ$  directions. Furthermore, as the former is also theoretically larger, it is difficult to clearly distinguish the effects of the seam. The yield stress of the material is approximately 410 MPa, but in the outer bending direction (negative direction of the stress in Figure 7), linearity with the flatness is observed within a range where this value is greatly exceeded.

Based on the measurements of the change of the external diameter (flatness) in the  $0^\circ$  to  $180^\circ$  directions, the section deformation when the flatness was 8 mm is  $M_i = 1.7 \cdot 10^5 \text{ N}\cdot\text{m}$  if  $2e_i = 0.8$  is substituted in equation (4) to obtain  $M_i$ . Substituting this value of  $M_i$  in equations (1), (2), and (3) to calculate the stress distribution, circumferential stress and longitudinal stress in Figure 8 are obtained. The symbols  $\square$  and  $\bullet$  represent the stress distribution obtained by the strain gauges. The theoretical equation calculates the stress distribution by inputting the stress values at the average wall thickness and the smallest wall thickness, but there is little difference between these in either the longitudinal direction or the circumferential direction. The peak of the circumferential stress appears almost at the  $0^\circ$  location, and the peak of the longitudinal stress is observed near  $20^\circ$ . In both cases, the stress calculated from the flatness and the stress calculated from the strain gauges agree very closely.

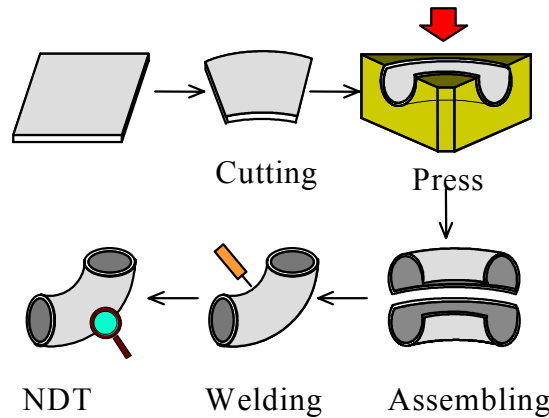


Figure 5: Welded elbow.

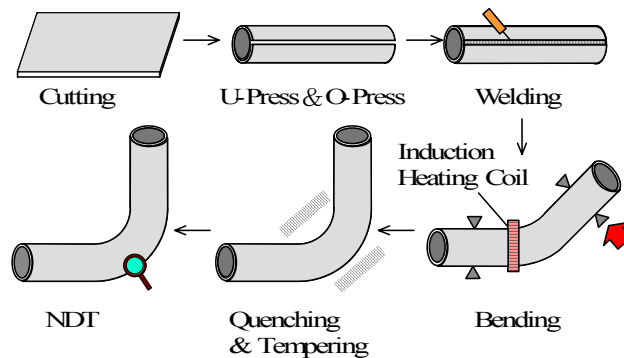


Figure 6: Induction pipe bend.

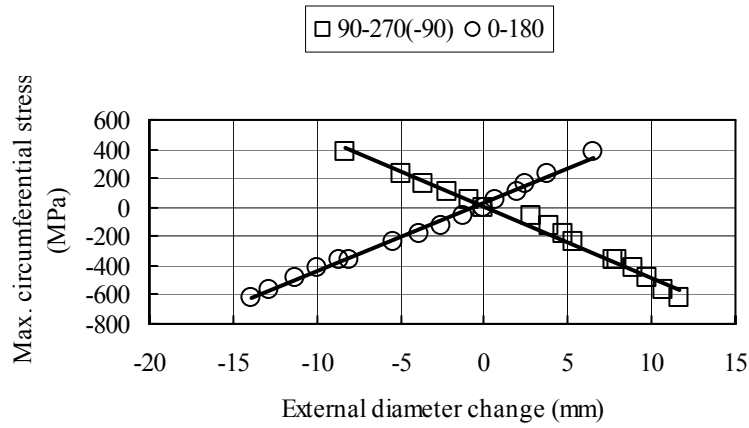


Figure 7: Relationship of change of external diameter with the maximum stress.

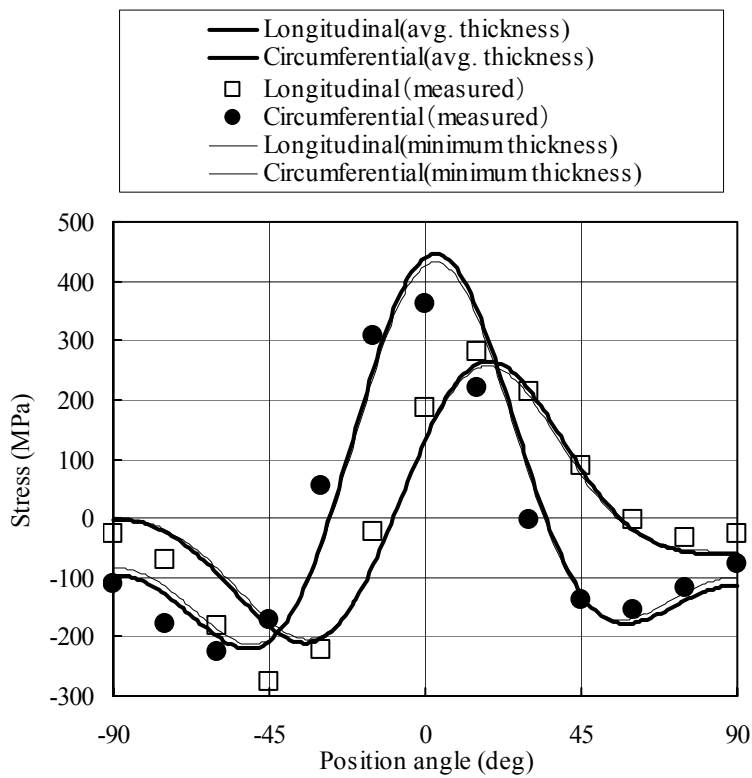


Figure 8: Comparison of the stress distribution calculated from the flatness with the stress distribution measured by strain gauges.

(b) Induction pipe bend. Figure 9 shows the relationship of the change in the external diameter

with the maximum stress of an induction pipe bend. The yield stress of the material is about 450 MPa, but the maximum negative stress fell below the yield stress in terms of the safety of the equipment. Within this range, the relationship of the flatness with the maximum circumferential stress was almost linear. A comparison with the theory is made for the case when flatness is 7.4 mm. Substituting  $e_i = 0.74/2$  in equation (4) gives  $M_i = 5.3 \cdot 10^5 \text{ N}\cdot\text{m}$ , which is then substituted in

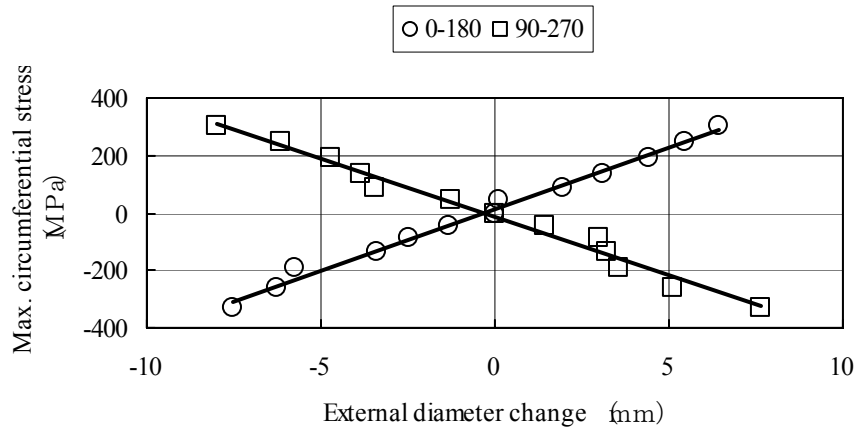


Figure 9: Relationship of change of external diameter with the maximum stress.

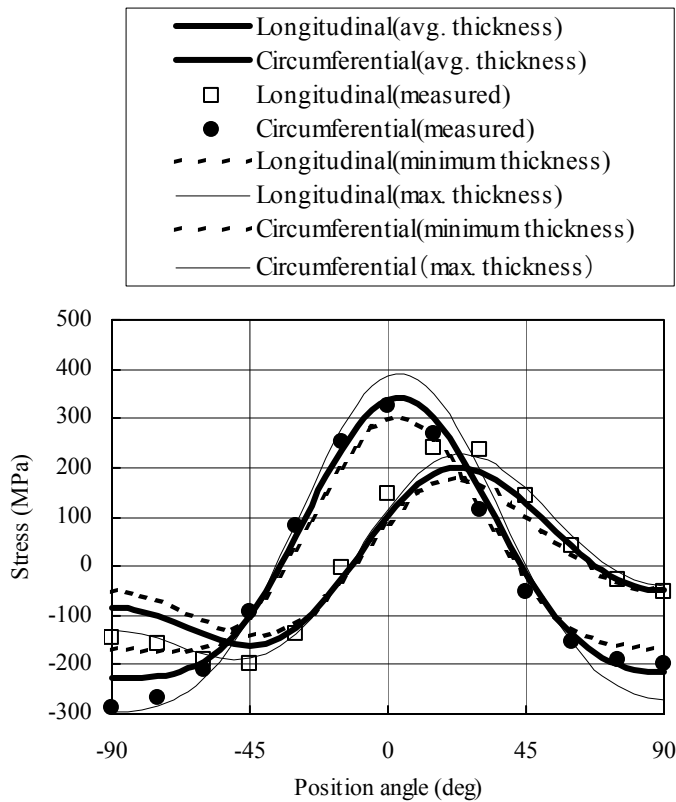


Figure 10: Comparison of the stress distribution calculated from the flatness with the stress distribution measured by strain gauges.

equations (1), (2), and (3) to calculate the stress distribution as shown in Figure 10. The effects of the wall thickness are slightly more marked than in the case of the welded elbow. In the circumferential direction, the estimated average wall thickness is closest to the measured values, and in the longitudinal direction, the estimated maximum wall thickness is closest to the measured values. In both cases, the stress estimated from the flatness closely agrees with the measured value.

The maximum stress during action by in-plane bending is produced in the circumferential direction. If the location where it is produced at this time is considered to be nearly  $0^\circ$ , equation (6) can be derived.

$$\sigma_{c\max} \approx \frac{3\lambda Ee}{20R(1-\nu^2)} \frac{(d_1 + 10d_2 + 35d_3)}{(d_1 + 2d_2 + 3d_3)} \quad (6)$$

**Conclusions:** It has been revealed that the stress distribution produced in a bent pipe during action by in-plane bending can be accurately represented by the theory of Rodabaugh-George. Test results have confirmed that even under stress within the elastic range, a change in diameter that can be measured with calipers is produced. The results of estimating stress from the flatness using the proposed equation and comparing it with measured stress have shown that it is possible to estimate the maximum stress with sufficient precision for practical use. Furthermore, tests have shown that because there is a material whose relationship of diameter change with maximum stress is linear until about 1.5 times the yield stress of the material, there is high possibility that the proposed method can be applied to a wide range of stress diagnoses.

Application of this method is premised on understanding the diameter change of the bent pipe caused by external force, but as a method of finding flatness, it is not necessary to perform a measurement from the outside surface of a pipe. Recently, a method of inspecting the inside surface of a pipe by passing an inspection pig through the pipe has occasionally been used. A profile pig that measures the shape such as the internal diameter inside such a pig is now in practical use. Therefore, this method can be combined with shape measurement data for practical application.

**Acknowledgement:** The author would like to acknowledge and thank Mr. Sakai of JFE Engineering Corporation for his assistance with the testing.

#### References:

- [1] S. Iimura : Simplified mechanical model for evaluating stress in pipeline subject to settlement, JCBM, Elsevier, Vol.18, Issue6, 2004, pp.119-129.
- [2] S. Iimura and Y. Sakai, Non-destructive method for measurement of stress in bent pipes, 3<sup>rd</sup> Int. Conf. Emerging Technologies in Non-Destructive Testing, Greece, pp.219-224 (2003)
- [3] Von Karman, Uber die Formänderung dünnwandiger rohre, insbesondere federnder ausgleichrohre, Zeitschrift des Vereines deutscher Ingenieure, Z. VDI, 55, pp.1889-1895(1911)
- [4] Rodabaugh, E. C., and George, H. H., Effect of internal pressure on flexibility and stress intensification factors of curved pipe or welding elbows, Trans. ASME, Vol.79, pp.939-948. (1957)